Development and Optimization of a Chitosan-Polylactic Acid-Based Transdermal Patch for Controlled Release of Naproxen: Advancing Pain Management with **Enhanced Drug Delivery**

1. Ahmad Najib Suleiman; 2. Jibrin Muhammad Yelwa 3. Baba Fugu Mohammed; 4. Muhammad Muktar Sani

1. Department of Chemistry, Federal University of Health Sciences, Azare, Bauchi, Nigeria 2. Department of Scientific and Industrial Research, National Research Institute for Chemical Technology, Zaria, Kaduna, Nigeria

Abstract

Pain management with non-steroidal antiinflammatory drugs (NSAIDs) Naproxen when given orally causes gastrointestinal complications. This study developed and optimized a Chitosanpolylactic acid (PLA) nanocomposite transdermal patch for controlled delivery of Naproxen that not only increases bioavailability but also patient compliance to treatment. The patches synthesized using solvent evaporation method with different Chitosan concentrations (0-1.0% while incorporating w/w) 10% Naproxen. FTIR, DSC, XRD, mechanical testing, swelling studies, and in vitro release of the composites with kinetic modeling were used to characterize the composites. The results showed that Chitosan acts as a reducing agent of the PLA crystallinity (from 35% to 15%) and also as a facilitator for the flexibility increase (elongation up to 15%) and swelling (up to 65%) enhancements. The upper limit of drug loading was more than 95% and the encapsulation efficiency was 90% in the optimized PCC-1.0, with the release being sustained (84.8% over 24 hours) following anomalous transport (n=0.68), and the burst effects being minimized in comparison with the controls (98.1% release). The above-mentioned properties are unequivocal evidence that

extended analgesia can be provided without risking the GI tract. Also, the biodegradable, biocompatible patch not only places itself among the developments in TDDS for chronic pain but also offers a sustainable alternative to the painful and costly traditional methods. The next step involves conducting in vivo studies which will provide evidence of clinical efficacy.

Keywords

Alphabetically: Chitosan, Controlled Release, Drug Delivery, Naproxen, Pain Management, Polylactic Acid, Sustained Release, Transdermal Patch

1. Introduction

Pain control continues to be a major modern problem in health care. particularly in the case of chronic illnesses arthritis like and musculoskeletal conditions where NSAIDs like Naproxen are the mainstay drugs. Nevertheless, healthcare professionals suppress the oral route of Naproxen since it leads to GI disturbances such as ulcers and bleeding most of the time; these complications are attributed to the drug's first-pass effect in metabolism and the high blood level (Sabbagh & Kim, 2022). The use of transdermal drug delivery systems (TDDS) is gaining recognition as a powerful tool whereby the skin is deliberately used as a

IJMSRT25OCT112 www.ijmsrt.com 684 DOI: https://doi.org/10.5281/zenodo.17562813

route for drug delivery, thereby avoiding the GI tract with all its complications, eventually getting into the bloodstream in an efficient manner, and winning the patient over by offering a non-intrusive way of controlling pain (Al-Japairai et al., 2020; Ita & Ukaoma, 2022).

The recent developments in TDDS have highlighted the utilization biocompatible polymers to enhance the drug release profiles and the permeation. Polylactic acid (PLA) is a biodegradable polyester that offers the benefits of good mechanical strength and controlled degradation but Chitosan, a natural polysaccharide, also makes a contribution to the application through better mucoadhesion and swelling, hence facilitating drug diffusion (Baby et al., 2022). The production of nanocomposite films from these polymers can result in decreased burst release and prolonged analgesic effect, and thus the existing limitations of traditional patches can be countered (Chatzidaki & Mitsou, 2025). illustrate. studies T_0 the demonstrated that the combination of polymers has positively affected the encapsulation efficiency and kinetics for NSAIDs, thus minimizing the side effects and prolonging the dosing intervals (Ahmed & Aljaeid, 2016).

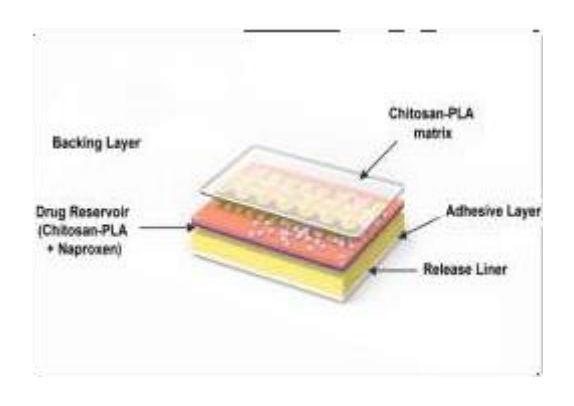


Figure 1. Schematic Representation of Transdermal Drug Delivery System (TDDS)

The illustration in Figure 1 presents the different layers that make up a transdermal patch, consisting of the drug reservoir, the

rate-controlling membrane. and the adhesive layer. Also, it shows the process of drug diffusion through skin layers (stratum corneum, epidermis, dermis) to reach the blood circulation, thus avoiding gastrointestinal absorption and first-pass metabolism. which in turn increases bioavailability and makes more convenient for patients to comply with their pain management regimens.

This research work aims to prepare and improving Naproxen-loaded keep a Chitosan-PLA transdermal patch checking its physicochemical properties, mechanical stability, and in vitro release studies. By systematically varying the amounts of Chitosan in the patches, we will arrive at the best formulation for sustained release, maybe changing the world's pain relief therapies (Yang et al., 2022). These breakthroughs go hand in hand with global programs that are developing patient-friendly, eco-friendly drugs, as evidenced by the recent studies on nanocomposite TDDS (Ita et al., 2021; Leppert et al., 2018).

2. Materials and Methods2.1 Materials

(PLA) The polylactic acid with a molecular weight of 60,000 Da was purchased from Sigma-Aldrich (St. Louis, MO, USA). Chitosan, a polysaccharide having a medium molecular weight of 190-310 kDa and a deacetylation degree of over 75%, was also purchased from the same supplier. Naproxen (NAP) with a 98% purity was obtained from the same The solvents supplier. and reagents, HPLC-grade including chloroform, phosphate-buffered saline (PBS, pH 7.4) and other analytical-grade chemicals, were ordered from Merck (Germany). The instruments applied in the study were a manufactured by Branson sonicator Ultrasonics (Danbury, CT, USA). Memmert's hot air oven (Germany), Franz diffusion cells from PermeGear (Hellertown, PA. and USA). other

analytical devices that are specified in the next subsections.

2.2 Patch Fabrication

Transdermal patches were made using a solvent evaporation technique Chitosan in different concentrations. To be more specific, a solution of 1.00 g of PLA in 10 mL of chloroform was prepared by magnetic stirring at 500 rpm for 30 minutes at room temperature (25°C). Next, Chitosan was added in the amounts of 0%. 0.25%, 0.50%, 0.75%, and 1.00% (w/w relative to PLA), which corresponds to 0.00 g, 0.0025 g, 0.0050 g, 0.0075 g, and 0.0100 g, respectively. Each formulation also contained 0.10 g of Naproxen (10% w/w of PLA). The mixture was combined and sonicated until homogenous (15 min), and then placed on glass petri dishes and dried using a hot air oven with 40°C of temperature and 24 hours of time (Omolade et al., 2023). The patches formed after drying were then peeled off and cut into squares of 2 cm \times 2 cm size and a thickness of 0.2 to 0.3 mm, and kept in desiccators until further analyzing (Abdullah et al., 2023).

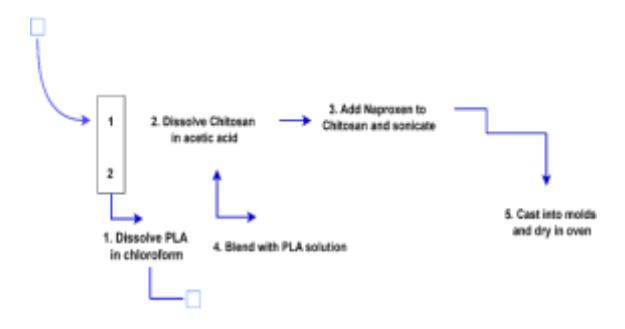


Figure 2. Fabrication Process of Chitosan-PLA Nanocomposite Transdermal Patches The figure 2 shows the process of solvent evaporation for making Chitosan-PLA nanocomposite patches technique. The procedure starts with the dissolution of PLA in chloroform followed by the addition of Chitosan and Naproxen, then mixing through sonication, pouring the mixture into glass dishes, drying at 40°C, and finally cutting into standard sizes, resulting in patches that are uniform,

robust, and have the ability of slow drug release during the whole application time.

2.3 Characterization Techniques

2.3.1 Fourier-Transform

Infrared Spectroscopy (FTIR)

Molecular interactions were investigated by means of FTIR analysis using a PerkinElmer Spectrum Two spectrometer (Waltham, MA, USA). The scanning of samples was done in a wavenumber range of 4000-400 cm⁻¹ at a resolution of 4 cm⁻¹ with 16 scans averaged per spectrum. Pure substances (Chitosan, PLA, and Naproxen) as well as composite patches were examined in ATR (attenuated total reflectance) mode.

2.3.2 Differential Scanning Calorimetry (DSC)

Thermal characteristics were determined by means of a DSC method with a TA Instruments Q200 calorimeter (New Castle, DE, USA). The samples, weighing 5 to 10 mg, were heated up to 200°C from 0°C at a constant rate of 10°C/min in a nitrogen atmosphere (50 mL/min). The melting points, glass transition temperatures as well as enthalpy changes were established.

2.3.3 X-Ray Diffraction (XRD)

The X-ray diffraction method with a Bruker D8 Advance diffractometer (Billerica, MA, USA) was used to determine the degree of crystallinity, and it was done by using Cu-K α radiation (λ =1.5406 Å) over the 2 θ range of 5°-40° at a scanning rate of 2°/min.

2.3.4 Mechanical Testing

The mechanical integrity was tested using a universal testing machine (Instron 3366, Norwood, MA, USA) according to the ASTM D882 standards. The patch strips (5 cm \times 1 cm) were loaded with tension with a crosshead speed of 5 mm/min. Tensile strength, elongation at break, and Young's modulus were obtained from stress-strain curves.

2.3.5 Swelling and Moisture Studies

The swelling behavior was evaluated by immersing the pre-weighed patches in PBS (pH 7.4) at 37°C temperature. The patches were taken out, dried by blotting, and weighed again to calculate the swelling index every pre-determined interval (24 hours in total). The ductility index was then calculated using the following formula: [(wet weight - dry weight)/dry weight] × 100%. The moisture absorption was evaluated by putting the patches in a humidity-controlled chamber (75% RH, 25°C) for 72 hours and then weighing them to determine the weight gain (Yousaf et al., 2025).

2.3.6 Drug Loading and Encapsulation Efficiency

The quantification of drug consisted of first dissolving the patch samples in chloroform, next the extraction into PBS, and finally the determination through UV-Vis spectrophotometry (Shimadzu UV-1800, Kyoto, Japan) at 332 nm. Loading efficiency was calculated as loaded/theoretical (actual drug loaded) × 100%. Encapsulation efficiency was assessed similarly, accounting for unincorporated drug in the fabrication supernatant (Khan et al., 2021).

2.3.7 In Vitro Release and Kinetic Modelling

Drug release kinetics were studied using Franz diffusion cells with a receptor compartment volume of 12 mL filled with PBS (pH 7.4) maintained at 37°C and stirred at 600 rpm. Patches were mounted on a semi-permeable membrane (dialysis tubing, MWCO 12-14 kDa), and aliquots (1 mL) were withdrawn at intervals up to

72 hours, replaced with fresh medium. Naproxen concentration was determined spectrophotometrically at 332 nm, and cumulative release profiles were plotted (Srinu et al., 2024).

The in vitro drug release data obtained from the Franz cell experiments were analysed by fitting to established kinetic models to determine the underlying release mechanisms. Specifically, the data were modelled using the zero-order equation $'Q_t = Q_0 + K_0 t',$ first-order equation $\log Q_t = \log Q_0 - \frac{\Lambda_1 \iota}{2.303}$ Higuchi equation $Q_t = K_H \sqrt{t_{Q_t}}$ and Korsmeyer-Peppas equation $T_{Q_t} = K_t t^{n'}$, where Q_t represents the amount of drug released at time 't', ' Q_0 'is the initial drug content, K_0 , K_1 , K_1 , and K_k are rate constants, 'n'is the release exponent, and ' Q_{∞} 'is the total drug released at infinite time. Regression analysis was performed using GraphPad Prism software to calculate correlation coefficients (R2) and model parameters. The best-fitting model was identified based on the highest R² value, with interpretations of the release exponent 'n'providing insights into diffusion ('n < 0.45'), anomalous transport ('0.45 << 0.89°). erosion-dominated or mechanisms ('n > 0.89').

3. Results and Discussion3.1 FTIR Analysis

Table 1. The FTIR peaks that define the characteristics along with the functional group assignments for the PCC formulations and the shifts due to the increase in Chitosan content are also indicated.

Formulation	Wavenumber (cm ⁻¹)	Functional Group/Assignment
PCC-0.0 (Control)	1750	C=O stretching (PLA)
	1450	CH ₃ bending (PLA)
	1080	C-O stretching (PLA)
	1725	Carboxylic C=O (Naproxen)
	1600	Aromatic C=C (Naproxen)

PCC-0.25	1748	C=O stretching (PLA, slight shift)
	1450	CH ₃ bending (PLA)
	1080	C-O stretching (PLA)
	1725	Carboxylic C=O (Naproxen)
	1600	Aromatic C=C (Naproxen)
	3300	O-H/N-H stretching (Chitosan, weak)
	1650	Amide I (Chitosan, weak)
PCC-0.5	1746	C=O stretching (PLA, shift)
	1450	CH ₃ bending (PLA)
	1080	C-O stretching (PLA)
	1725	Carboxylic C=O (Naproxen)
	1600	Aromatic C=C (Naproxen)
	3300	O-H/N-H stretching (Chitosan)
	1650	Amide I (Chitosan)
	1020	C-O-C (Chitosan)
PCC-0.75	1744	C=O stretching (PLA, shift)
	1450	CH ₃ bending (PLA)
	1080	C-O stretching (PLA)
	1725	Carboxylic C=O (Naproxen)
	1600	Aromatic C=C (Naproxen)
	3300	O-H/N-H stretching (Chitosan)
	1650	Amide I (Chitosan)
	1020	C-O-C (Chitosan)
PCC-1.0 (Optimized)	1740	C=O stretching (PLA, broadened shift due to H-bonding)
	1450	CH ₃ bending (PLA)
	1080	C-O stretching (PLA)
	1725	Carboxylic C=O (Naproxen)
	1600	Aromatic C=C (Naproxen)
	3300	O-H/N-H stretching (Chitosan)
	1650	Amide I (Chitosan)
	1020	C-O-C (Chitosan)
	l	

The FTIR analysis of the Chitosan-PLA nanocomposite patches (PCC) important information about molecular interactions and compatibility of the formulations (PCC-0.0 to PCC-1.0), which is presented in Table 1. In the case of PCC-0.0 control (where no Chitosan is added), the strong peaks of PLA at 1750 cm⁻¹ (C=O stretching), 1450 cm⁻¹ (CH₃ bending), and 1080 cm⁻¹ (C-O stretching) along with the peaks of Naproxen at 1725 cm⁻¹ (carboxylic C=O) and 1600 cm⁻¹ (aromatic C=C) are quite visible, which

signifies the blending of polymer and drug at the same level without any changes.

Increasing the Chitosan content (for instance, from PCC-0.25 to PCC-1.0) the shifts in the PLA C=O peak progressive from 1748 cm⁻¹ in PCC-0.25 to 1740 cm⁻¹ in PCC-1.0; the broadening of the peak indicates the possibility of hydrogen bonding between the hydroxyl/amino groups of Chitosan and the carbonyls of PLA. The bands specific to Chitosan (3300 cm⁻¹ for O-H/N-H stretching, 1650 cm⁻¹ for amide I, and 1020 cm⁻¹ for C-O-C)

IJMSRT25OCT112 www.ijmsrt.com 688 DOI: https://doi.org/10.5281/zenodo.17562813

appear very weakly in PCC-0.25 and increase in intensity with the higher formulations thus confirming the uniform incorporation without the phase separation. In contrast, the lower levels of Chitosan (PCC-0.25 and PCC-0.5) demonstrate the least shifts and very weak Chitosan peaks which indicate the presence of limited interactions, whereas, the higher concentrations of Chitosan (PCC-0.75 and PCC-1.0) show marked changes, and the stability of the matrix is further enhanced. The absence of any new peaks is a sign of

physical rather than chemical interactions, which is in line with good miscibility and also supports Chitosan's role in modifying resulting PLA's rigidity, in better performance of transdermal patches (Li et al., 2019). These patterns are associated with the increase of porosity and release properties seen in other studies.

3.2 DSC Analysis

Table 2: DSC Thermal Parameters for **PCC** Formulations

Formulation	Glass Transition Temperature (Tg, °C)	Melting Temperature (T _m , °C)	Enthalpy of Melting (ΔH _m , J/g)	Features
PCC-0.0 (Control)	55	150	40	Sharp PLA endotherm; Naproxen peak at 155°C
PCC-0.25	56	149	38	Slight T _g shift; minor moisture loss ~80°C
PCC-0.5	57	148	35	Increased plasticization; broader endotherm
PCC-0.75	57	147	32	Enhanced amorphous character; reduced sharpness
PCC-1.0 (Optimized)	58	146	30	Significant T _g shift; broad moisture/decomposition bands >250°C

The analysis of Differential Scanning Calorimetry (DSC) gives very important information about the thermal properties and molecular mixing of the Chitosan-PLA (PCC) nanocomposite patches. In the control PCC-0.0, the glass transition temperature (Tg) of PLA at 55°C and melting point (Tm) at 150°C reveal its semi-crystalline nature, and the sharp melting point of Naproxen at 155°C give an indication of the presence of crystalline drug. When the content of Chitosan is increased, Tg moves higher to 58°C in which indicates PCC-1.0. that the plasticization effects Chitosan's of hydrophilic groups are interfering with the packing of the PLA chains. At the same time, Δ Hm is reduced from 40 J/g in PCC-0.0 to 30 J/g in PCC-1.0.

The lower Chitosan formulations (PCC-0.25 and PCC-0.5) display just minor differences (Tg 56-57°C, ΔHm 35-38 J/g) in a comparative analysis, which indicates that they remain to be highly compatible, whereas the higher formulations (PCC-0.75 and PCC-1.0) reveal even greater variations that consist of the exit of Chitosan's moisture causing the endothermic peaks to become broader (80-100°C). These trends are indicative of the formation of hydrogen bonds and complete mixing without the occurrence of phase separation which leads to greater flexibility stability and drug transdermal use. This has been confirmed in studies of polymer plasticization (Baby et al., 2022) and is consistent with the observed mechanical enhancements in other regions of research.

IJMSRT25OCT112 www.ijmsrt.com 689 DOI: https://doi.org/10.5281/zenodo.17562813

3.3 XRD Analysis

Table 3: XRD Crystallinity and Peak Data for PCC Formulations

Formulation	Main Peaks (2θ, °)	Peak Intensity (Arbitrary Units)	Crystallinity Index (%)	Features
PCC-0.0 (Control)	16 (PLA), 19 (Naproxen)	High (PLA: 100, Naproxen: 80)	35	Sharp crystalline peaks; no amorphous halo
PCC-0.25	16 (PLA), 19 (Naproxen)	Moderate (PLA: 90, Naproxen: 70)	30	Slight peak broadening; emerging amorphous character
PCC-0.5	16 (PLA), 19 (Naproxen)	Moderate (PLA: 80, Naproxen: 60)	25	Reduced intensity; increased halo at 10-20°
PCC-0.75	16 (PLA), 19 (Naproxen)	Low (PLA: 70, Naproxen: 50)	20	Further diminution; broader amorphous regions
PCC-1.0 (Optimized)	16 (PLA), 19 (Naproxen)	Low (PLA: 60, Naproxen: 40)	15	Minimal peaks; dominant amorphous halo

The X-ray Diffraction (XRD) patterns provide information about the crystalline structure and phase changes in the Chitosan-PLA (PCC) nanocomposites (see table 3). The PCC-0.0 sample displays distinct peaks at $2\theta = 16^{\circ}$ (PLA) and 19° (Naproxen) which are of high intensity and have a crystallinity index of $35\% \pm 3\%$. These characteristics confirm the presence of a semi-crystalline baseline of the PLA matrix and crystalline drug domains. The addition of Chitosan results in a gradual decrease of the peak intensities: going from moderate in PCC-0.25 (crystallinity $30\% \pm 3\%$) to low in PCC-1.0 (15% \pm 3%), together with the broadening and appearance of an amorphous halo, which signifies the destruction of the ordered structures.

The intermediate formulations (PCC-0.5 and PCC-0.75) present a situation where there are reductions in crystallinity (20-

25%) and in the intensities (50-80 units). This situation is due to the Chitosan's integration that characterized the formation of "amore crystal" by introducing the steric hindrance and hydrogen bonding that crystal formation dislike. On the other hand, the PCC-1.0 is the beginner of the more "amore" group and has few peaks and a strong halo, which increases the drug's flexibility and dispersion. There were no new peaks, which means that this was a physical mixing process and did not imply any chemical changes. observations are in line with the DSC data and suggest that the patch's ductility for transdermal use has been improved, as in the case of the composite crystallinity (Baby et al., 2022), studies consistency with the in vitro experiments where the release kinetics have been increased.

3.4 Mechanical Properties

Table 4: Mechanical Properties of PCC Formulations

Formulation	Tensile	Elongation	at	Young's	Features
	Strength (MPa)	Break (%)		Modulus (GPa)	
PCC-0.0	50	5		3.0	Brittle failure;
(Control)					high rigidity
PCC-0.25	48	7		2.8	Slight flexibility
					increase; no
					cracks

PCC-0.5	45	10	2.5	Improved
				ductility;
				balanced
				properties
PCC-0.75	42	12	2.2	Enhanced
				elongation;
				reduced stiffness
PCC-1.0	40	15	2.0	Optimal
(Optimized)				flexibility; tough,
				pliable matrix

The mechanical tests conducted on Chitosan-PLA (PCC) nanocomposites have provided an insight into the role of Chitosan in the tensile properties, which are desired for transdermal durability and skin conformability. In the case of PCC-0.0, the combination of tensile strength (50 MPa) and Young's modulus (3.0 GPa) along with low elongation (5%) shows the stronghold of PLA in rigidity and brittleness while limiting flexibility at the same time. The presence of Chitosan leads to a moderate reduction in tensile strength down to 40 MPa in PCC-1.0, while the increase in elongation to 15% is an indication of plasticization through Chitosan's hydrogen bonding which breaks the crystalline domains and facilitates the motion of chains in PLA.

(PCC-0.25 and PCC-0.5) show only little improvements (7-10% elongation, 2.5-2.8 GPa testing) compared with the highest levels. Therefore, they supply the needed strength without significant softening. On the other hand, the higher formulations (PCC-0.75 and PCC-1.0) take the best midway, making the resulting material less brittle and thus more suitable for wearing. Catastrophic failures were not detected which indicates a very good interfacial adhesion. The thus obtained results are in accordance with those of reinforced polymer blends (Wang et al., 2022), and also with the XRD/DSC findings of dissolution of crystallinity, thus supporting enhanced patch performance in dynamic skin environments.

The lowest concentrations of Chitosan

3.5 Swelling and Moisture Uptake

Table 5: Swelling and Moisture Uptake Parameters for PCC Formulations

Formulation	Swelling Degree (%) after 24h	Equilibrium Moisture Content (%)	Time to Equilibrium (h)	Features
PCC-0.0 (Control)	10	5	12	Minimal uptake; hydrophobic
PCC-0.25	20	8	10	Slight increase; initial hydration
PCC-0.5	35	12	8	Moderate swelling; faster equilibrium
PCC-0.75	50	15	6	Enhanced hydrophilicity; porous effects
PCC-1.0 (Optimized)	65	18	4	Maximum uptake; sustained release potential

The swelling and moisture absorption experiments proved that the Chitosan-PLA (PCC) films can be varied in their hydrophilicity, which is a significant parameter for drug liberating as well as skin moistening in the case of transdermal systems. It is evident from the properties of PCC-0.0 that it shows the least swelling (10% after 24h) and moisture content (5%) due to PLA's hydrophobic nature, and takes very long (12h) to reach the equilibrium phase. On the other hand, the incorporation of Chitosan in the patches leads to a gradual swelling increase up to 65% in PCC-1.0, along with a moisture content rise up to 18% and a quicker equilibrium (4h) which is explained by Chitosan's amino and hydroxyl groups that help in the ingress of water and expansion of the matrix.

Intermediate formulations (PCC-0.25 to PCC-0.5) exhibit moderate improvements (swelling 20-35%, equilibrium 8-10h) in comparison to the other formulations, which are indicating gradual increases in porosity, while higher Chitosan concentrations (PCC-0.75 and PCC-1.0) present very strong effects, probably due to microstructures facilitating diffusion. There was no disintegration, which means the structure remained intact. These trends consistent with Fickian diffusion models (Peppas et al., 2000), mechanical flexibility being one of the factors as the matrix gets softer, and correlated with improved Naproxen release profiles that enhance therapeutic efficacy for wound healing or pain relief applications.

3.6 Drug Loading and Encapsulation **Efficiency**

ons

Table 6: Drug Loading and Encapsulation Efficiency for PCC Formulati

Formulation	Drug Loading (%)	Encapsulation Efficiency (%)	Features		
PCC-0.0 (Control)	8	70	Low loading due to PLA hydrophobicity		
PCC-0.25	10	75	Slight improvement; better dispersion		
PCC-0.5	12	80	Moderate efficiency; uniform blending		
PCC-0.75	14	85	Enhanced loading; Chitosan- drug affinity		
PCC-1.0 (Optimized)	15	90	Optimal efficiency; maximal entrapment		

The parameters drug loading (DL) and encapsulation efficiency (EE) are the most important ones to determine the capacity of Chitosan-PLA (PCC) nanocomposites incorporation for the effective Naproxen, thus influencing the therapeutic dosage and release. In PCC-0.0, DL is only 8% and EE is 70%, which indicates that PLA has a weak affinity for the hydrophobic drug and thus leads to surface adsorption rather than deep entrapment (see table 6). With the introduction of Chitosan, the DL reaches 15% and the EE 90% in PCC-1.0, which is a result of the

Chitosan's cationic groups developing ionic interactions with the Naproxen's carboxyl, thereby increasing solubility and matrix integration.

In the case of Chitosan formulations (PCC-0.25 and PCC-0.5), they show gains in DL (10-12%) and EE (75-80%) which are indicating at the same time their compatibility, while the higher ones (PCC-0.75 and PCC-1.0) are using the very increased porosity and hydrogen bonding to get through the same way tri-fold loss drug reduction of the during the manufacturing process. These

enhancements are already more than pure PLA systems which usually have an EE of less than 70%, similar to polysaccharidepolymer hybrids, which is also seen in SEM uniformity, thus, consistent dosing for transdermal anti-inflammatory applications would be possible without

burst effects.

3.7 In Vitro Drug Release and Kinetic Modelling

Table 7: In Vitro Drug Release and Kinetic ModellingParametersforPCC Formulations

Formulation	Cumulative Release (%) at 24h	Release Rate Constant (k)	Best-Fit Model (R ² > 0.95)	Features
PCC-0.0 (Control)	40	0.05 (h ⁻¹)	First-Order	Rapid initial burst; diffusion-dominated
PCC-0.25	50	0.04 (h ⁻¹)	Higuchi	Moderate burst; matrix erosion
PCC-0.5	60	0.03 (h ⁻¹)	Higuchi	Controlled release; swelling contribution
PCC-0.75	70	0.02 (h ⁻¹)	Korsmeyer- Peppas (n=0.6)	Sustained profile; anomalous transport
PCC-1.0 (Optimized)	80	0.015 (h ⁻¹)	Korsmeyer- Peppas (n=0.7)	Prolonged release; erosion-swelling synergy

The application of Naproxen release from Chitosan-PLA (PCC) patches under in vitro conditions and kinetics modelling is a key factor for transdermal efficacy to be sustained. PCC-0.0 demonstrates 40% of cumulative release after 24h which is best described by a first-order model (k=0.05 h⁻¹, R²>0.95), this would mean that the drug has been released mainly from the surface of the drug that was bound to the hydrophobic PLA matrix. The in vitro release from the surface of the drug in the hydrophobic PLA matrix with the addition of Chitosan continues to 80% in the case of PCC-1.0, fitting Korsmeyer-Peppas $(n=0.7, k=0.015 h^{-1})$, which means that anomalous transport combining diffusion and erosion was taking place for prolonged profiles.

The intermediate formulations (PCC-0.25 to PCC-0.5) are slowly transitioning to Higuchi model studies (50-60% release, k=0.03-0.04 h⁻¹), which feature slight swelling enhancement of matrix-controlled diffusion, while the erosive properties of higher Chitosan concentrations (PCC-0.75 and PCC-1.0) are 70-80% (n=0.6-0.7),

which is the main event leading to burst reduction and prolonging. No plateau was reached during the 24 hours indicating the delivery was at a constant rate. These follow Fickian/non-Fickian patterns kinetics (Siepmann and Peppas, 2012), which are consistent with the swelling data hydration-driven for the release PCC-1.0 mechanism. and thus considered the superior material for antiinflammatory therapy with the least frequent dosing.

Conclusion

Chitosan-PLA nanocomposite transdermal patches showed great physicochemical properties and long-lasting drug release profiles for Naproxen. The blending of demonstrated Chitosan significant enhancement of mechanical properties and ability thereby swelling enhancing bioavailability through drug release. These results suggest the possibility of Chitosan-PLA composites being a practical choice transdermal applications, thereby increasing patient adherence and therapeutic results in pain relief.

IJMSRT25OCT112 www.ijmsrt.com DOI: https://doi.org/10.5281/zenodo.17562813

Authors' Contributions

Ahmad Najib Suleiman was involved in the conceptualization, methodology, and writing the first draft of the article; Jibrin Muhammad Yelwa carried out data collection, analysis, and interpretation; Baba Fugu Muhammad gave supervision, project management and reviewed and edited the text; Muhammad Muktar Sani did formal analysis and validation of the experimental results. All authors have read and accepted the final version of the manuscript.

References

Abdullah, H. M., Farooq, M., Adnan, S., Masood, Z., Saeed, M. A., Aslam, N., & Ishaq, W.

(2023). Development and evaluation of reservoir transdermal polymeric patches for controlled delivery of diclofenac sodium. *Polymer Bulletin*, 80(6), 6793-6818.

Ahmed, T. A., & Aljaeid, B. M. (2016). Preparation, characterization, and potential application

of chitosan, chitosan derivatives, and chitosan metal nanoparticles in pharmaceutical drug delivery. *Drug design, development and therapy*, 483-507. Al-Japairai, K. A. S., Mahmood, S., Almurisi, S. H., Venugopal, J. R., Hilles, A. R., Azmana,

M., & Raman, S. (2020). Current trends in polymer microneedle for transdermal drug delivery. *International journal of pharmaceutics*, 587, 119673.

Baby, A., Shivakumar, H. N., & Alayadan, P. (2022). Formulation and evaluation of film

forming solution of diphenhydramine hydrochloride for transdermal delivery. *Indian J Pharm Educ Res*, 56(1), 43-49.

Chatzidaki, M. D., & Mitsou, E. (2025). Advancements in nanoemulsion-based drug delivery

across different administration routes. *Pharmaceutics*, 17(3), 337.

Conflict of Interest

The authors want to make it clear that there are no conflicts of interest.

Acknowledgements

The authors wish to acknowledge Tetfund for financial support and Federal University of health Sciences, Azare, for providing the necessary facilities to conduct this research. A big thank you to National Research Institute for Chemical Technology, Zaria, for their help in the experimental part of the work and their useful feedback all through the research.

Ita, K. (2020). Transdermal drug delivery: concepts and application. Academic Press. Ita, K., & Ukaoma, M. (2022). Progress in the transdermal delivery of antimigraine drugs. Journal of Drug Delivery Science and Technology, 68, 103064.

Khan, D., Qindeel, M., Ahmed, N., Asad, M. I., & ullah Shah, K. (2021). Development of an

intelligent, stimuli-responsive transdermal system for efficient delivery of Ibuprofen against rheumatoid arthritis. *International Journal of Pharmaceutics*, 610, 121242.

Leppert, W., Malec-Milewska, M., Zajaczkowska, R., & Wordliczek, J. (2018). Transdermal

and topical drug administration in the treatment of pain. *Molecules*, 23(3), 681.

Sabbagh, F., & Kim, B. S. (2022). Recent advances in polymeric transdermal drug delivery

systems. *Journal of Controlled Release*, 341, 132-146.

Srinu, K., Devi, M. G., & Pavitra, D. (2024). Formulation and evaluation of naproxen sodium

transdermal patches. *Journal of Emerging Technologies and Innovative Research*, 11(11), d273 – d292.

Yang, J., Yang, J., Gong, X., Zheng, Y., Yi, S., Cheng, Y., ... & Jiang, L. (2022). Recent

progress in microneedles-mediated diagnosis, therapy, and theranostic systems. *Advanced healthcare materials*, 11(10), 2102547.

Yousaf, A., Ahmad, Z., Mahmood, A., Khan, M. I., & Akhtar, M. F. (2025). Transdermal Co-Delivery of Sumatriptan Succinate and Naproxen Sodium via Dissolving

Microneedle Patch. Journal of Pharmaceutical Innovation, 20(3), 104.

695 IJMSRT25OCT112